Nanoscience and Nanotechnology 2015, 5(4): 89-96
DOI: 10.5923/j.nn.20150504.03

Green Synthesis of Gold Nanoparticles Using Cumin Seeds and Gum Arabic: Studying Their Photothermal Efficiency

Thanaa I. Shalaby*, Rasha S. Shams El-Dine, Suzan A. Abd El-Gaber

Medical Biophysics department, Medical Research Institute, Alexandria University, Egypt

Abstract Biocompatible gold nanoparticles have gained considerable attention in recent years for potential applications in nanomedicine. This work is aimed at exploring the green synthesis of gold nanoparticles using cumin seeds with gum Arabic as a simple, non-toxic, eco-friendly 'green material'. The growth of nanoparticles was monitored by UV-Vis spectrophotometer and complemented with Transmission Electron Microscopy (TEM), X-ray Diffraction (XRD) and Fourier Transform Infrared Spectroscopy (FTIR). The UV-Vis spectrum of Cumin-Au NPs showed a peak at 540 nm corresponding to the surface Plasmon resonance band (SPR) of gold nanoparticles. FTIR spectroscopy indicated the involvement of biomolecules present in cumin seeds and gum Arabic in the synthetic process. The TEM micrograph of Cumin-Au NPs showed spherical nanoparticles with an average size of 5.5 nm. The crystalline nature of Cumin-Au NPs was confirmed by X-ray diffractometer. Cumin-Au NPs showed remarkable stability in different buffers including saline, histidine, cysteine and BSA solutions. The photothermal efficiency of cumin-Au NPs was investigated when added to HeLa cells and irradiated with Nd: YAG laser (532 nm, 150 mW). Cell survival was monitored by trypan blue exclusion assay. The photothermal efficiency of Cumin-Au NPs increased as the laser energy increased. It is clear from result that, green synthesized Au-NPs can be used as novel class of photothermal agents using laser at low power in the visible region.

Keywords Green synthesis, Gold nanoparticles Cumin and gum Arabic, Photothermal efficiency, YAG laser

1. Introduction

The application of nanoscale materials and structures, usually ranging from 1 to 100 nanometers (nm), is an emerging area of nanoscience and nanotechnology. Nanomaterials may provide solutions to technological and environmental challenges in the areas of solar energy conversion, catalysis, medicine, and water treatment [1, 2]. This increasing demand must be accompanied by "green" synthesis methods. In the global efforts to reduce generated hazardous waste, "green" chemistry and chemical processes are progressively integrating with modern developments in science and industry.

Nanomaterials often show unique and considerably changed physical, chemical and biological properties compared to their macro scaled counterparts [3]. Additionally, metal nanoparticles have a surface Plasmon resonance absorption in the UV–Visible region. The surface Plasmon band arises from the coherent existence of free electrons in the conduction band due to the small particle size [4]. Due to the strong surface Plasmon absorption, gold nanoparticles offer great potential in photothermal therapy applications. It has been found that the strong absorbed radiation is converted efficiently into heat on a picosecond time domain due to electron-phonon and phonon-phonon processes [5]. Thus, upon the laser irradiation at the surface Plasmon absorption band, the nanoparticles absorb photon energy and then immediately transfer into heat energy. If the nanoparticles are incorporated or incubated with biomolecules; cells or tissues, this heat energy will cause a sharp increase on the local temperature around the nanoparticles and thus cause the damage of the surrounding materials. This photothermal destruction can be used for cancer therapy. Compared to other nanoparticles, gold nanoparticles have great advantages in cancer applications due to their easy preparation, efficient bioconjugation, potential noncytotoxicity, tunable and enhanced scattering and absorption properties [6].

Generally, metal nanoparticles can be prepared and stabilized by physical and chemical methods; the chemical approach, such as chemical reduction, electrochemical techniques, and photochemical reduction is most widely used [7]. Studies have shown that the size, morphology, stability and properties (chemical and physical) of the metal nanoparticles are strongly influenced by the experimental

* Corresponding author:
th_shalaby@yahoo.com (Thanaa I. Shalaby)
Published online at http://journal.sapub.org/nn

conditions, the kinetics of interaction of metal ions with reducing agents, and adsorption processes of stabilizing agent with metal nanoparticles [8]. Hence, the design of a synthesis method in which the size, morphology, stability and properties are controlled has become a major field of interest [9].

There is increasing pressure to develop clean, nontoxic, and environmentally benign synthetic technologies. Recently biosynthetic methods employing either microorganism [10, 11] or plant extracts have emerged as environmentally sustainable alternatives to chemical synthetic procedures. In recent years plant-mediated biological synthesis of nanoparticles is gaining importance due to its simplicity and eco-friendliness. Several plants have been successfully used for efficient and rapid extracellular synthesis of gold nanoparticles [12-14].

The aim of the present study is to synthesize biocompatible gold nanoparticles (Cumin-Au NPs) using cumin seeds and gum Arabic and studying their characterization, in vitro stability and their photothermal efficiency to kill tumor cells.

2. Materials and Methods

2.1. Materials

For the synthesis of gold nanoparticles, Trihydrated tetrachloroauric acid ($HAuCl_4.3H_2O$, 99.9%) from Sigma Aldrich, Cumin seeds and gum Arabic were purchased from organic grocery sources. Deionized water was used for all solution preparations and experiments. Before the reduction process all glass wares were cleaned in aqua regia (3 parts HCl, 1 part HNO_3), rinsed with deionized water, and then oven dried.

2.2. Synthesis of Gold Nanoparticles Using Cumin and Gum Arabic

Cumin seeds were washed to remove any impurities and dried under sunlight for a week to remove the moisture completely. For reduction of $AuCl_4$- ions, 12 mg of gum Arabic was added to 6 mL of deionized water (DI). The reaction mixture was stirred continuously at 45°C for 10 minutes. To the stirring mixture 100 µl of 0.1M $HAuCl_4.3H_2O$ (in DI water) was added followed by (300 mg) of cumin seeds. The color of the mixture turned from pale yellow to purple-red within 5 minutes indicating the formation of gold nanoparticles. The reaction mixture was stirred for an additional 15 minutes at room temperature. The gold nanoparticles thus formed were separated from residual cumin seeds immediately using 5 micron filter.

2.3. Characterization of the Prepared Gold Nanoparticles

2.3.1. UV-Visible Spectrum Analysis

UV-Vis spectroscopy analyses of Cumin-gold nanoparticles were recorded on a single beam spectrophotometer (Unicam UV-Vis spectrometry model UV5-220), using quartz cell of 1 cm path length and deionized water as the reference solvent at room temperature. UV-Vis spectrum is an indication of surface Plasmon resonance (SPR) that depicts the size and distribution of nanoparticles.

2.3.2. Transmission Electron Microscopy (TEM) Analysis

Transmission electron microscopy was used to study the size and morphology of the prepared Au-NPs. One droplet of gold colloidal solution was placed onto a carbon coated cupper grid and allowed to dry in air naturally at room temperature then examined using TEM (JEOL-100 CX).

2.3.3. Fourier Transform Infrared Spectroscopic Analysis

After the complete reduction of AuCl4-ions using cumin seeds and gum Arabic, solution was centrifuged at 3000 rpm for 15 min and the resulting suspension was re-dispersed into 20 ml of deionized water, the process of centrifugation and re-dispersion was repeated three times to make nanoparticles free from bioorganic compounds present in the solution. There after the purified suspension was completely dried in lyophilizer. The pellets were prepared by grinding 4-8 mg of lypholized samples with 200 mg of potassium bromide and compressed using Shimatzu compressor (Japan), the pellets were then fixed on holder to be examined. The spectrum was scanned over the wave number range of 4000 to 400 cm^{-1}.

2.3.4. X-ray Diffraction Analysis

X-ray diffraction (XRD) was carried out with an X-ray diffractometer (Shimadzu, XRD-7000, Maxima, Japan). Samples were irradiated with monochromatized Cu Kα radiation and analyzed between 5 and 100° (2 θ). The voltage and current used were 30 kV and 30 mA, respectively.

The crystalline gold nanoparticle was calculated from the width of the XRD peaks, using the Debye-Scherrer formula:

$$\mathbf{D = 0.9\lambda / \beta \cos\theta}$$

where D is the mean crystallite diameter of the nanoparticles, λ is the wavelength of the X-ray radiation source, β is the angular full width half maxima (FWHM) of the XRD peak at the diffraction angle (Bragg's angle) 2θ.

2.4. *In vitro* Stability Studies of Gold Nanoparticles

In vitro stability of Cumin-Au-NPs was tested in the presence of 10% NaCl, 0.5% cysteine, 0.2 M histidine and 0.5% bovine serum albumin (BSA). The stability of gold nanoparticles was monitored by UV- visible spectra in different buffer media for different time intervals (1 hr, 24 hrs and 7 days). The Plasmon resonance band at ~540 nm confirmed the retention of nanoparticulates in all the above mixtures.

2.5. Cell Culture

HeLa cell lines (human cervix adenocarcinoma) obtained

from MRI, Semouha. Alex. University, Egypt, were maintained in DMEM (Dulbecco's Modified Eagle Medium) supplemented with 10% fetal bovine serum (FBS) and 1% penicillin-streptomycin in physiological conditions (37°C and 5% CO_2). Exponentially growing cells were adjusted to a concentration of 2×10^4 cells/ml. Cells were seeded at 20,000 cells/well in a 24-well tissue culture plates; the medium solution was added to plates to make sure to cover at least the plate bottom. The cells were homogeneously dispersed in the whole well plate by gently swirling.

2.6. Photothermal Study

For laser irradiation experiments, HeLa cells were cultured in triplicates at density of 20,000 cells/well. HeLa cells lines were incubated at 37°C for 15 min to stabilize temperature. Plates were transferred to laminar flow hood as sterile work area. Gold NPs with concentration of 100µg/ml were added to each well, plate was incubated with nanoparticles for 3 h at 37°C. Thereafter, the cells were washed thoroughly in phosphate buffer saline (PBS, pH 7.4) to remove any surface bound or uncoordinated gold nanoparticles. For laser irradiation experiments, HeLa cells were irradiated by laser radiation delivered from a Nd:YAG laser system (λ = 532 nm, 150 mW). A collimated laser beam with spot size of 5 mm was used to irradiate the cells. The irradiation times were 10, 20 and 40 s, with energy densities of 7.65, 15.2 and 30.55 J/cm^2, then plates were incubated for 24 hours. Cells incubated in culture medium without the Au NPs served as the control group in each experiment. Cell viability was measured by trypan blue exclusion assay. Cell morphology changes were studied under phase contrast microscope and transmission electron microscope.

2.7. Cell Count with Trypan Blue Staining

After laser irradiation, the dead cells were floating in the culture medium in the wells; these cells were removed and stored in a tube. The live cells were stuck down firmly on the tissue culture plate; these cells were detached by trypsinization with 0.5 ml trypsin for 2-3 min and were also collected. Both the floating cells and the attached cells were stained with Trypan blue and were count using hemocytometer under inverted microscope (Zeiss Axiovert 25). The live or dead cells number fraction is the number of the live or dead cells divided by the total cells number respectively.

2.8. Cellular Uptake of AuNPs and Morphological Changes

After 3 hours incubation with the Au NPs, HeLa cells were washed by PBS, trypsinized, and then collected in 15 ml centrifuge tubes. Cells were washed by sodium cacodylate buffer, fixed with 2.5% glutaraldehyde buffered in sodium cacodylate for 4 hour, then transferred to micro-centrifuge tubes, and washed with sodium cacodylate buffer for 3 times. After that, the cells were stained in 1% osmium tetroxide for 30 minutes, washed with sodium cacodylate buffer for 3 times. Pre-warmed agar solution (60°C) was added onto the cell pellets. The cell pellets were cut into four cubes and transferred into small glass bottles, then dehydrated through a series of alcohol concentrations (50%, 70%, 90%, and 100%), followed by propylene oxide, and finally infiltrated with 1:1 epoxy resin/propylene oxide mixture for overnight. The cell blocks were subsequently filtrated with fresh epoxy resin for 1 hour at 37°C, with the help of vacuum oven, then were embedded in fresh epoxy resin in plastic capsules and polymerized at 60°C overnight. Ultrathin sections were cut using a LKB ultramicrotome, mounted on carbon-coated copper grids. The sections were post-stained with uranyl acetate and lead citrate. The cells were imaged under TEM (JEOL-100 CX) to study cellular uptake of Au NPs and the morphological changes.

3. Results and Discussion

3.1. Characterization of Gold Nanoparticles

3.1.1. UV-Vis. Spectrophotometer

The synthesized Au nanoparticles were confirmed by visual observation. The color was changed into pink-ruby red due to reduction of gold ions. It was well known that Au nanoparticles exhibits pink-ruby red color in aqueous solution due to excitation of surface plasmon vibrations (Fig.1). The synthesized Au nanoparticles using cumin seeds and gum Arabic were detected by UV-Vis spectrophotometer at various nm. Absorption spectra of gold nanoparticles formed in the reaction mixture at different nm (350-700 nm), the particle has increasingly sharp absorbance maximum peak at 540nm and gradually decreased while nanometer increased (Fig. 2). It is clear from the figure that nanoparticles solution of gold was stable for more than one week.

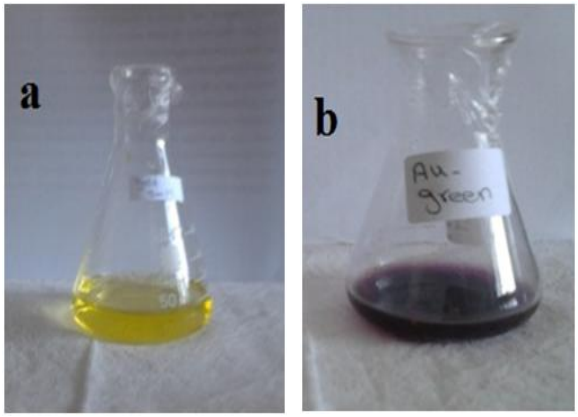

Figure 1. Gold solution, (a) before reduction, (b) after reduction

3.1.2. Qualitative Assessment by TEM

The morphology and size of the formed gold nanoparticles were determined by TEM. As revealed from micrograph, the small and mostly spherical-shaped nanoparticles produced with cumin seeds and gum Arabic, within the size range of

3.96- 8.84 nm, (Fig. 3), is presumed to be due to the presence of high concentrations of reducing chemicals in the cumin seeds. Cumin-Au NPs are homogeneously distributed, this may due to the presence of gum Arabic which stabilize the particles and prevent their aggregations.

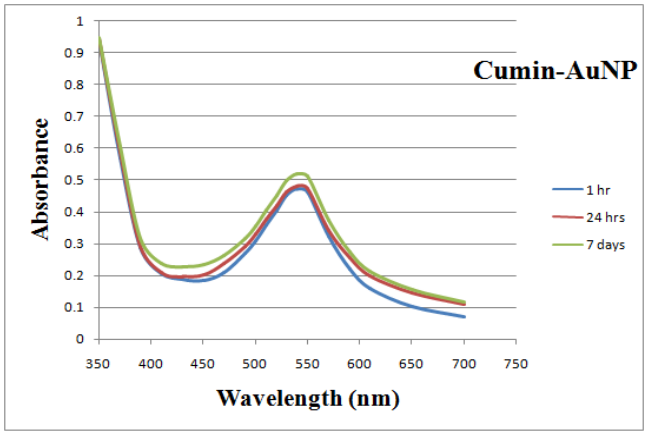

Figure 2. UV-Vis absorption spectra recorded for gold nanoparticles synthesized by cumin and gum Arabic as function of time

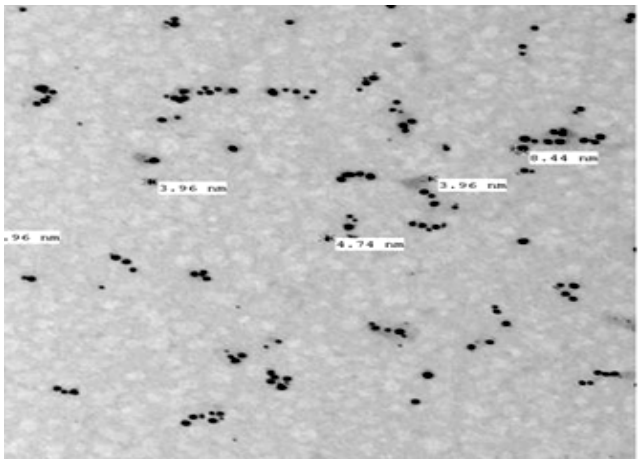

Figure 3. TEM micrograph of gold nanoparticles biosynthesized by cumin and gum Arabic

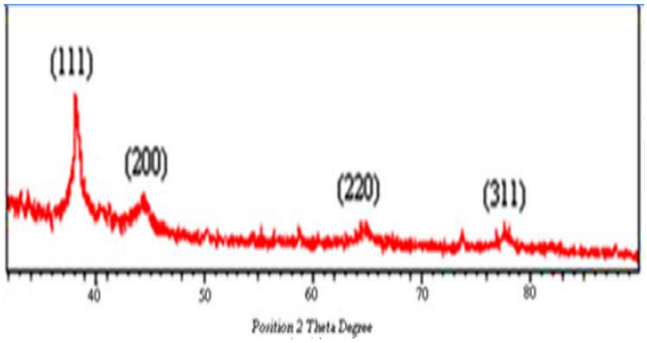

Figure 4. XRD pattern for green synthesized Au-NPs using cumin and gum Arabic

3.1.3. Confirmation of Au-NPs

Figure (4) shows the XRD patterns of Cumin-Au nanoparticles. Four prominent crystalline peaks at 37° (2θ), 45° (2θ), 64° (2θ) and 78 (2θ) were detected. A number of Bragg reflections corresponding to the (111), (200), (220) and (311) sets of lattice planes are observed which may be indexed based on the face centered cubic (fcc) structures of gold. The typical XRD pattern revealed that gold nanoparticles formed using cumin seeds and gum Arabic was essentially crystalline in nature. The average particle diameter for the crystalline particle as determined by Scherre's formula, using the half widths of the most intense XRD peaks was 5.48 ± 0.79 nm.

3.1.4. Formation Mechanism by FTIR

FTIR spectrum of Au nanoparticles synthesized using cumin seeds and gum Arabic was shown in (Fig. 5). FTIR measurements were carried out to identify the possible biomolecules responsible for capping and efficient stabilization of the metal nanoparticles. The spectrum peaks represents different functional groups of adsorbed biomolecules on the surface of the nanoparticles and also indicates the influence of organic moieties on the formation of Au nanoparticles and for stabilization in the aqueous medium. The peak at 3424 cm^{-1} assigned to the primary amines. The band 2924 cm^{-1} may be assigned to secondary amines, the absorption peak at 1650 cm^{-1} was N–H stretching of amide I, which was characteristic of the stretch mode of the carbonyl group coupled to the amide linkage. This suggested that proteins bind to Au-NPs through free amine groups. The peaks at 1650 cm^{-1}, 1402 cm^{-1} and 1117 cm^{-1} show the presence of flavonoids present in cumin seeds. This clearly shows that the freely water soluble flavonoids present in the seed extract could have been adsorbed on the surface and the same may be induced in the catalytic reduction of Au^{3+} ions to Au^{0} nanoparticles.

3.2. *In Vitro* Stability Study for Cumin Gold Nanoparticles

For biomedical applications that require lower concentrations of Au-NPs, it is critical that dilution of Au-NPs does not alter the chemical and photo-physical properties. Additionally, different Au-NPs synthesized by different methods must be stable under an *in vitro* environment that mimics in *vivo* conditions for any potential biomedical applications. Au-NPs are known to aggregate in the presence of electrolytes. [15] The stability of Cumin -AuNPs was evaluated by monitoring the SPR band in the presence of 10% NaCl, 0.5% cysteine, 0.2 M histidine and 0.5% BSA that mimic biological environments. UV-Vis spectra of gold solution ware measured as a function of time variation for each substance, Fig. (6 a-d). The Plasmon wavelength in all the above formulations showed no change or minimal shifts of ~1–5 nm. The Plasmon resonance band at ~540 nm confirmed the retention of nanoparticulates in all the above mixtures. This retention indicates that the Au-NPs are intact, and thereby demonstrate excellent in vitro stability in biological fluids.

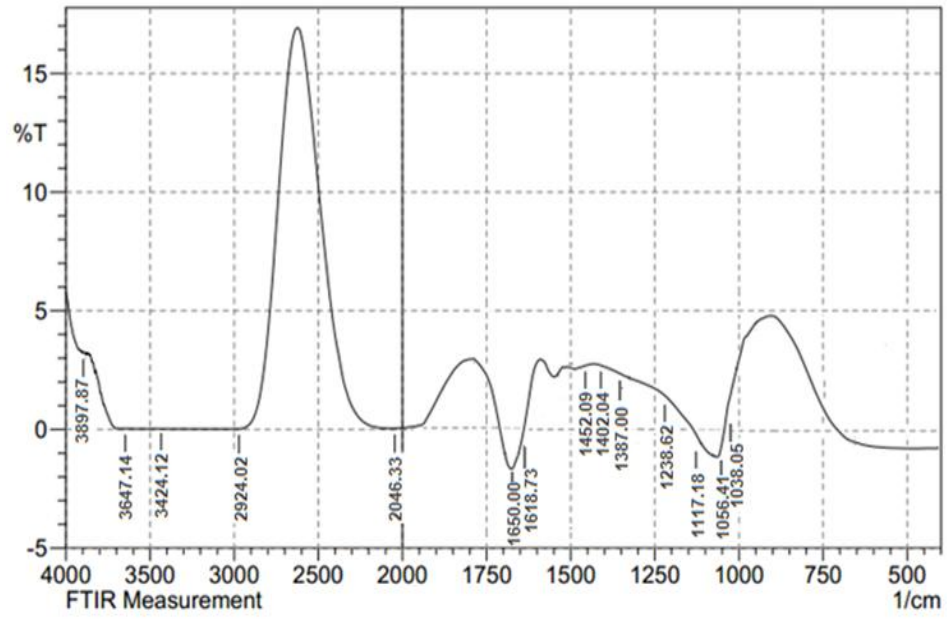

Figure 5. FT-IR spectrum of Au NPs using cumin and gum Arabic

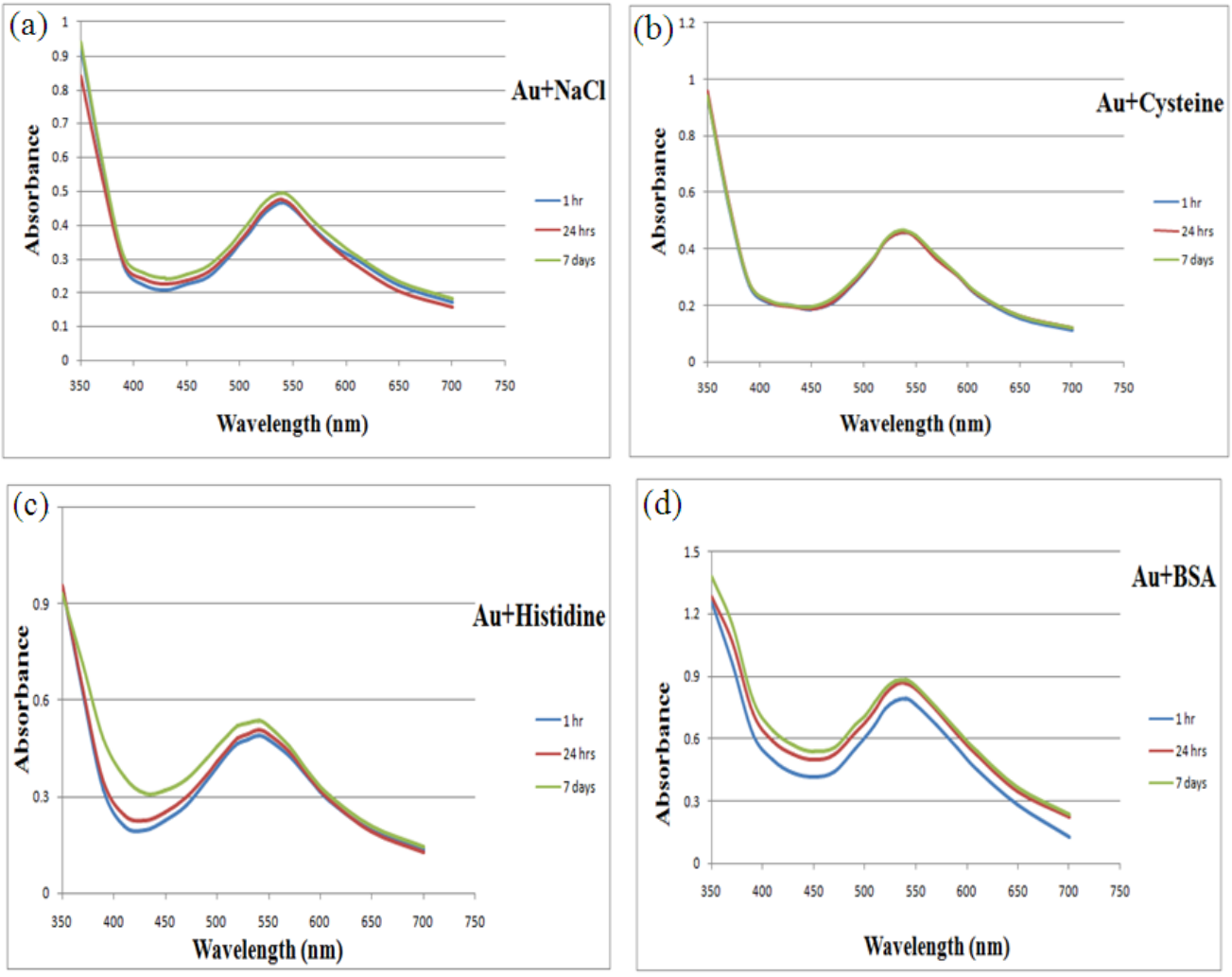

Figure 6. UV-Vis absorption spectra of cumin-AuNPs showing in vitro stability of the nanoparticles in different media, 10% NaCl (a), 0.5% cysteine (b), 0.2M histidine (c) and 0.5% BSA (d) as function of time

3.3. Photothermal Efficiency of Gold Nanoparticles

The excitation of Plasmon resonance in a gold nanoparticle results in significant enhancement of its absorption cross-section. Thus, for efficient laser heating of the nanoparticles, the wavelength of the incident irradiation should coincide with the position of the Plasmon resonance. After incubation of HeLa cells with gold nanoparticles, much more cells were killed during irradiated with Nd: YAG laser (532 nm, 150 mW) and the efficiency increased as the laser energy value increased. No photothermal destruction was observed for HeLa cells irradiated with laser even at high energy (30.55 J/cm^2) without gold nanoparticles. When HeLa cells incubated with gold nanoparticles without laser exposure, negligible number of dead cells was observed. After laser irradiation, the number fraction of cells incubated with Au NPs and irradiated with different laser energies become significantly smaller than that of control and the dead cell number fraction were much larger accordingly as shown in Fig.7.

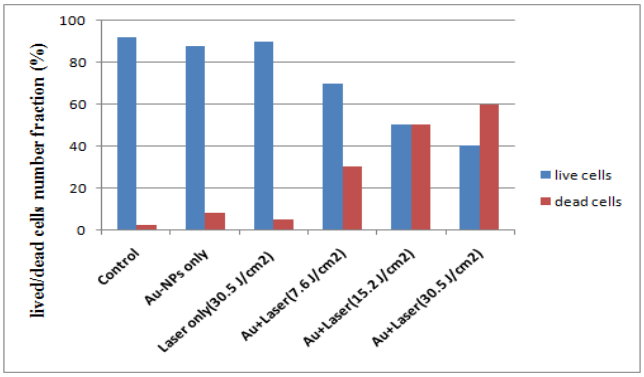

Figure 7. Live and dead cell number fractions for HeLa cell samples incubated with AuNPs for 24 h and irradiated with laser of different energies

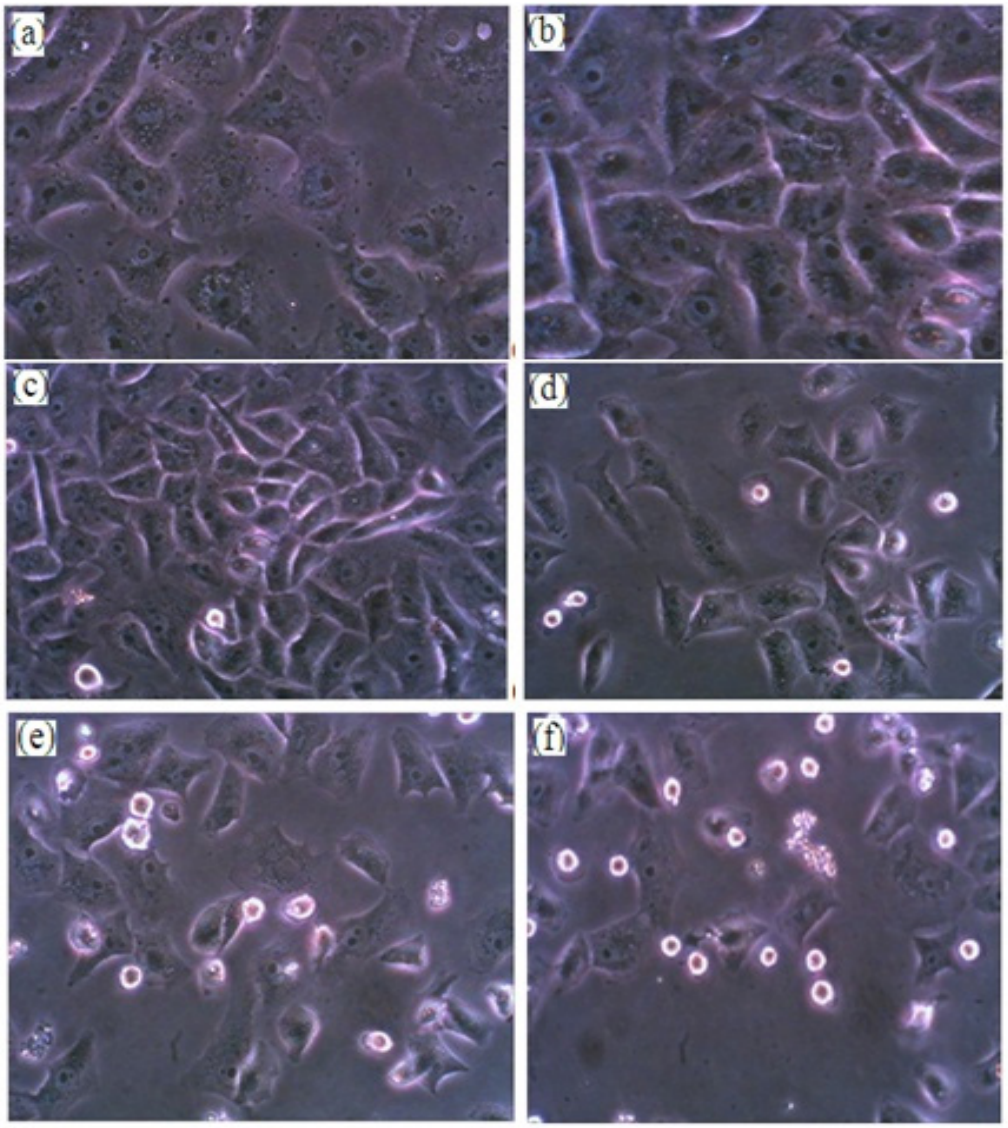

Figure 8. Phase contrast microscope images of HeLa cells, (a) without gold nanoparticles and no laser exposure, (b) exposed only to laser energy of 30.55 J/cm^2, (c) incubated with gold nanoparticles with no laser exposure, (d) incubated with colloidal gold (100 ug/ml) and exposed to laser energy of 7.65 J/cm^2, (e) incubated with colloidal gold and exposed to laser energy of 15.2 J/cm^2, (f) incubated with colloidal gold and exposed to laser energy of 30.55 J/cm^2. (32x)

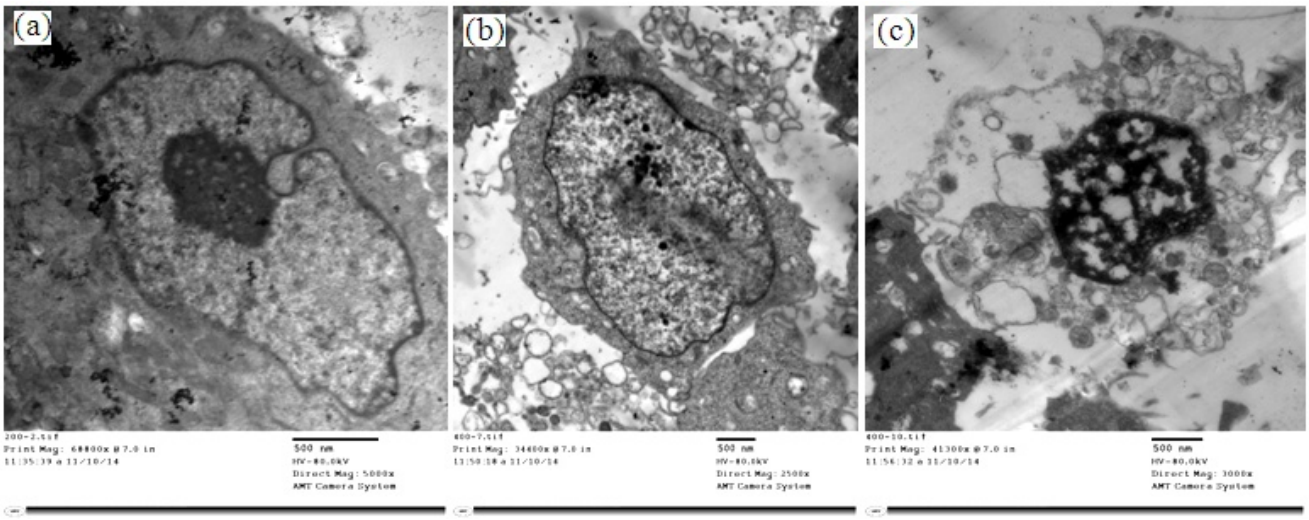

Figure 9. HeLa cells incubated with 100 µg/ml cumin Au NPs without laser exposure (a&b) while (c) showed the cell morphological changes when incubated with Au NPs and exposed to laser energy of 30.55 J/cm^2, scale bar =500 nm

For further confirmation, the morphology of the cells incubated with Au-NPs and irradiated with laser was examined under phase contrast microscopy. HeLa cells without Au-NPs were taken as control for this experiment (Fig.8a). To test the photothermal stability of the cells, HeLa cells were exposed to laser light at highest laser energy value (30.55 J/cm^2), it is obvious that even at high laser energies, no death was observed (Fig. 8b). HeLa cells incubated with gold nanoparticles and then exposed to Nd:YAG laser (532 nm, 150 mW) for different times 0, 10, 20 and 40 sec, showed different percent of death cells with different laser energies (0, 7.65, 15.2 and 30.55 J/cm^2) as shown in Fig. 8(c-f), respectively. Since HeLa cells are an adherent cell line, they normally grow flat and stuck down firmly on the tissue culture flask. After irradiation with laser, the cells change shape, becoming round and more refractile (brighter) under phase contrast microscopy. The dead cells detach from the tissue culture flask and float in the medium.

3.4. Cellular Uptake of AuNPs and Morphological Changes

The uptake of Au NPs into HeLa cells can be visualized in TEM images. Figure (9) shows the attachment of Au NPs on the cell surface and the intertwining between the cell microvilli. It can be observed that some Au NPs were internalized into the HeLa cytoplasm forming the vacuoles (b). On the basis of these observations, the uptake of GNPs is consistent with receptor-mediated endocytosis [16, 17]. Previously, it was reported that the uptake of Au NPs can result in cell morphological changes, disruption of the cell membrane, disorganized cell cytoskeleton and eventual cell death as shown in Fig. (9-c). [18].

4. Conclusions

Plants or their extracts can be efficiently used in the synthesis of gold nanoparticles as a greener route. Control over the shape and size of nanoparticles seems to be very easy with the use of plants. In the present study we found that cumin seeds with gum Arabic can be good source for synthesis of gold nanoparticles. This approach toward the synthesis of gold nanoparticles has many advantages such as, ease with which the process can be scaled up, economic viability, etc. Applications of such eco-friendly nanoparticles in medical applications, makes this method potentially exciting for the large-scale synthesis of other inorganic materials (nanomaterials). We demonstrate the ability of using gold nanoparticles as effective absorber of laser radiation in-vitro photothermal cancer cell therapy. The cancer cell destruction method described in this study is an effective photothermal cancer therapy technique which can be effective for in vivo cancer therapy.

REFERENCES

[1] Hu M., Chen J.Y., Li Z.Y., Au L., Hartland G.V., Li X.D., Marquez M., Xia Y.N. 2006. Gold nanostructures: engineering their plasmonic properties for biomedical applications. Chemical Society Reviews; 35: 1084-1094.

[2] Huang X.H., Jain P.K., El-Sayed I.H., El-Sayed M.A. 2007. Gold nanoparticles: Interesting optical properties and recent applications in cancer diagnostic and therapy .Nanomedicine; 2: 681-693.

[3] Sharma VK, Yngard RA, Lin Y. 2009. Silver nanoparticles: Green synthesis and their antimicrobial activities. Advances in Colloid and Interface Science; 145: 83–96.

[4] Eustis S., El-Sayed M.A. 2006. Why gold nanoparticles are more precious than pretty gold: noble metal surface plasmon resonance and its enhancement of the radiative and nonradiative properties of nanocrystals of different shapes. Chemical Society Reviews; 35: 209-217.

[5] Link S., El-Sayed M.A. 2003. Optical properties and ultrafast dynamics of metallic nanocrystals. Annu. Rev Phys Chem; 54:

331-366.

[6] Huang W.Y., Qian W., El-Sayed M.A., Ding Y., Wang Z.L. 2007. Effect of the Lattice Crystallinity on the Electron-Phonon Relaxation Rates in Gold Nanoparticles. Journal of Physical Chemistry C; 111: 10751–10757.

[7] Frattini A, Pellegri N, Nicastro D, De Sanctis O. 2005. Effect of amine groups in the synthesis of Ag nanoparticles using aminosilanes. Mater Chem Phys; 94: pp.148

[8] Sengupta S, Eavarone D, Capila I, Zhao GL, Watson N, Kiziltepe T, Sasisekharan R. 2005. Temporal targeting of tumor cells and neovasculature with a nanoscale delivery system. Nature; 436: 568 – 572.

[9] Wiley B, Sun Y, Xia Y. 2007. Synthesis of silver nanostructures with controlled shapes and properties. Acc Chem Res; 40:1067.

[10] Sawle B.D., Salimath B., Deshpande R., Bedre M.D., Prabhakar B.K., Venkataraman A. 2008. Biosynthesis and stabilization of Au and Au-Ag alloy nanoparticles by fungus, Fusarium semitectum. Science and Technology of Advanced Materials; 9: 035012-035017.

[11] Husseiny M.I., El-Aziz M.A., Badr Y., Mahmoud M.A. 2007. Biosynthesis of gold nanoparticles using Pseudomonas aeruginosa. Spectrochimica Acta Part A; 67: 1003-1006.

[12] Shankar S.S., Rai A., Ahmad A., Sastry M. 2005. Controlling the optical properties of lemongrass extract synthesized gold nanotriangles and potential application in infrared-absorbing optical coatings. Chem Mater; 17: 566-572.

[13] Huang J, Li Q, Sun D, Lu Y, Su Y, Yang X, et al. 2007. Biosynthesis of silver and gold nanoparticles by novel sundried Cinnamomum camphora leaf. Nanotechnology; 18: 105104-105114.

[14] Shankar S.S., Rai A., Ahmad A., Sastry M. 2004. Rapid synthesis of Au, Ag, and bimetallic Au core–Ag shell nanoparticles using neem (Azadirachta indica) leaf broth. J Colloid Interf Sci.; 275: 496-502.

[15] Wang G., Sun W. 2006. Optical limiting of gold nanoparticle aggregates induced by electrolytes. The journal of physical chemistry B; 110: 20901-20905.

[16] Connor E.E., Mwamuka J., Gole A.; Murphy C.J.; Wyatt, M.D. 2005. Gold Nanoparticles Are Taken Up by Human Cells but Do Not Cause Acute Cytotoxicity. Small; 1: 325-327.

[17] Paciotti G. F., Myer L., Weinreich D., Goia D., Pavel N., McLaughlin R.E., Tamarkin L. 2004. Colloidal Gold: a Novel Nanoparticle Vector for Tumor Directed Drug Delivery. Drug Deliv; 11: 169-183.

[18] Uboldi C., Bonacchi D., Lorenzi G., Hermanns M.I.; Pohl C., Baldi G., Unger R.E.; Kirkpatrick C.J. 2009. Gold Nanoparticles Induce Cytotoxicity in the Alveolar Type-II Cell Lines A549 and NCIH441. Part Fibre. Toxicol; 6: 18.